<Electronic Supplementary Information>

Coordinating nature of M_6L_{12} double-stranded macrocycles: co-ligand competition of perchlorate, water, and acetonitrile depending on metal(II) ions

Seonghyeon An,[a] Jihun Han,[a] Dongwon Kim,[a] Haeri Lee*[b] and Ok-Sang Jung*[a]

[a]*Department of Chemistry, Pusan National University, Busan 46241, Republic of Korea.*

Fax: (+82) 51-5163522; Tel: (+82) 51-5103240; E-mail: oksjung@pusan.ac.kr

[b]*Department of Chemistry, Hannam University, Daejun 34054, Republic of Korea.*

E-mail: haeri.lee@hnu.ac.kr

Table S1 Crystallographic data

	$[Mn_6(ClO_4)_4(CH_3CN)_2(H_2O)_6L_{12}]8ClO_4\cdot CH_3CN\cdot 7C_7H_8$	**$[Co_6(ClO_4)_4(CH_3CN)_7(H_2O)L_{12}][Co_6(ClO_4)_4(CH_3CN)_5(H_2O)_3L_{12}]16ClO_4\cdot 6C_7H_8$**	**$[Cu_6(ClO_4)_8(CH_3CN)_4L_{12}]4ClO_4\cdot 5C_7H_8$**	**$[Zn_6(ClO_4)_4(CH_3CN)_2(H_2O)_6L_{12}]8ClO_4\cdot CH_3CN\cdot 5C_7H_8$**	**$[Cl@Cu_2(ClO_4)_2L_4]ClO_4\cdot 4C_7H_8$**
Formula	$C_{295}H_{389}Cl_{12}Mn_6N_{27}O_{54}Si_{12}$	$C_{544}H_{713}Cl_{24}Co_{12}N_{60}O_{100}Si_{24}$	$C_{566}H_{728}Cl_{24}Cu_{12}N_{56}O_{96}Si_{24}$	$C_{281}H_{373}Cl_{12}N_{27}O_{54}Si_{12}Zn_6$	$C_{108}H_{136}Cl_4Cu_2N_8O_{12}Si_4$
M_w	6269.43	11924.82	12139.44	6147.74	2119.48
Cryst. sys.	Monoclinic	Monoclinic	Orthorhombic	Monoclinic	Monoclinic
Space group	*P*2/*n*	$P2_1$	*Iba*2	*P*2/*n*	$P2_1/n$
a (Å)	25.370(5)	26.225(5)	35.019(7)	25.489(5)	16.9088(8)
b (Å)	34.527(7)	30.532(6)	45.420(9)	34.525(7)	36.984(2)
c (Å)	43.510(9)	43.614(9)	46.291(9)	43.539(9)	17.1187(7)
V (Å^3)	37952(13)	34555(12)	73628(25)	38133(13)	10701.8(8)
Z	4	2	4	4	4
ρ (g cm^{-3})	1.097	1.146	1.095	1.071	1.315
μ (mm^{-1})	0.359	0.658	0.504	0.759	0.605
R_{int}	0.2017	0.0465	0.0753	0.0498	0.1079
GoF on F^2	1.192	1.022	0.912	1.824	1.081
R_1 [$I>2\sigma(I)$][a]	0.2040	0.0913	0.0577	0.1910	0.0620
wR_2 (all data)[b]	0.5800	0.2955	0.1731	0.5596	0.1833

[a] $R_1 = \Sigma||F_o| - |F_c||/\Sigma|F_o|$, [b] $wR_2 = (\Sigma[w(F_o^2 - F_c^2)^2]/\Sigma[w(F_o^2)^2])^{1/2}$

Table S2 Selected bond length (Å) and angle (°)

$[Mn_6(ClO_4)_4(CH_3CN)_2(H_2O)_6L_{12}]8ClO_4 \cdot CH_3CN \cdot 7C_7H_8$		$[Co_6(ClO_4)_4(CH_3CN)_7(H_2O)L_{12}][Co_6(ClO_4)_4(CH_3CN)_5(H_2O)_3L_{12}]16ClO_4 \cdot 6C_7H_8$			
O(1A)-Mn(1A)	2.155(10)	Co(1A)-N(1)	2.16(1)	Co(1B)-N(37)	2.129(8)
N(1)-Mn(1A)	2.119(7)	Co(1A)-N(2)	2.162(9)	Co(1B)-N(39)	2.171(9)
O(1)-Mn(2A)	2.427(7)	Co(2A)-O(53)	2.106(8)	Co(2B)-O(81)	2.128(7)
O(2A)-Mn(2A)	2.319(13)	Co(2A)-O(1A)	2.187(8)	Co(2B)-O(1B)	2.216(7)
O(5)-Mn(3A)	2.307(15)	Co(3A)-O(82)	2.075(7)	Co(3B)-N(58)	2.131(9)
O(3A)-Mn(3A)	2.478(13)	Co(3A)-O(5A)	2.221(7)	Co(3B)-O(5B)	2.217(7)
O(4A)-Mn(1B)	2.222(7)	Co(4A)-N(4)	2.150(10)	Co(4B)-N(56)	2.117(8)
Mn(1B)-N(2)	2.188(9)	Co(4A)-N(3)	2.162(9)	Co(4B)-N(38)	2.170(8)
O(9)-Mn(2B)	2.233(6)	O(9A)-Co(5A)	2.262(8)	Co(5B)-N(61)	2.128(9)
O(5A)-Mn(2B)	2.198(6)	Co(5A)-O(83)	2.101(9)	Co(5B)-O(9B)	2.182(8)
O(13)-Mn(3B)	2.261(6)	Co(6A)-N(59)	2.15(1)	Co(6B)-N(57)	2.128(8)
O(6A)-Mn(3B)	2.132(6)	Co(6A)-O(13A)	2.234(7)	Co(6B)-O(13B)	2.183(7)
N(1)-Mn(1A)-O(1A)	173.3(5)	N(1)-Co(1A)-N(2)	174.5(4)	N(37)-Co(1B)-N(39)	179.2(4)
O(2A)-Mn(2A)-O(1)	174.5(4)	O(53)-Co(2A)-O(1A)	176.1(4)	O(81)-Co(2B)-O(1B)	171.3(3)
O(5)-Mn(3A)-O(3A)	162.3(5)	O(82)-Co(3A)-O(5A)	179.2(3)	N(58)-Co(3B)-O(5B)	177.5(4)
N(2)-Mn(1B)-O(4A)	178.3(3)	N(4)-Co(4A)-N(3)	178.2(4)	N(56)-Co(4B)-N(38)	179.3(4)
O(5A)-Mn(2B)-O(9)	173.9(3)	O(83)-Co(5A)-O(9A)	175.7(4)	N(61)-Co(5B)-O(9B)	173.7(4)
O(6A)-Mn(3B)-O(13)	171.5(3)	N(59)-Co(6A)-O(13A)	177.5(4)	N(57)-Co(6B)-O(13B)	179.2(4)

$[Cu_6(ClO_4)_8(CH_3CN)_4L_{12}]4ClO_4 \cdot 5C_7H_8$		$[Zn_6(ClO_4)_4(CH_3CN)_2(H_2O)_6L_{12}]8ClO_4 \cdot CH_3CN \cdot 5C_7H_8$		$[Cl@Cu_2(ClO_4)_2L_4]ClO_4 \cdot 4C_7H_8$	
Cu(1)-N(1)	2.361(8)	O(1A)-Zn(1A)	2.15(2)	Cu(1)-N(1C)	2.026(4)
Cu(1)-O(17)	2.595(6)	N(1)-Zn(1A)	2.196(9)	Cu(1)-N(1D)	2.030(3)
Cu(2)-O(1)	2.469(7)	O(1)-Zn(2A)	2.29(1)	Cu(1)-N(1B)	2.042(3)
Cu(2)-O(21)	2.379(6)	Zn(2A)-O(2A)	2.29(2)	Cu(1)-N(1A)	2.047(3)
N(2)-Cu(3)	2.401(8)	O(5)-Zn(3A)	2.38(1)	Cu(1)-O(1)	2.379(3)
Cu(3)-O(5)	2.544(7)	Zn(3A)-O(3A)	2.15(1)	Cu(1)-Cl(1)	2.661(1)
N(3)-Cu(4)	2.343(7)	Zn(1B)-O(1B)	2.111(6)	Cl(1)-Cu(2)	2.672(1)
Cu(4)-O(25)	2.611(8)	Zn(1B)-N(2)	2.239(8)	Cu(2)-N(2B)	2.037(4)
Cu(5)-O(29)	2.405(7)	O(9)-Zn(2B)	2.251(6)	Cu(2)-N(2D)	2.038(3)
Cu(5)-O(9)	2.451(8)	Zn(2B)-O(2B)	2.148(6)	Cu(2)-N(2C)	2.040(3)
N(4)-Cu(6)	2.449(8)	O(13)-Zn(3B)	2.272(6)	Cu(2)-N(2A)	2.045(4)
Cu(6)-O(13)	2.495(6)	Zn(3B)-O(3B)	2.135(7)	Cu(2)-O(5)	2.409(4)
N(1)-Cu(1)-O17	176.27(3)	O(1A)-Zn(1A)-N(1)	177.7(6)	N(1D)-Cu(1)-N(1B)	179.3(2)
O(1)-Cu(2)-O(21)	178.58(4)	O(2A)-Zn(2A)-O(1)	167.1(6)	N(1C)-Cu(1)-N(1A)	178.2(1)
N(2)-Cu(3)-O(5)	170.94(4)	O(3A)-Zn(3A)-O(5)	175.6(4)	O(1)-Cu(1)-Cl(1)	174.0(1)
N(3)-Cu(4)-O(25)	176.11(3)	O(1B)-Zn(1B)-N(2)	178.0(3)	N(2B)-Cu(2)-N(2D)	177.8(1)
O(9)-Cu(5)-O(29)	178.62(4)	O(2B)-Zn(2B)-O(9)	178.2(3)	N(2C)-Cu(2)-N(2A)	178.6(1)
N(4)-Cu(6)-O(9)	170.19(3)	O(3B)-Zn(3B)-O(13)	173.7(3)	O(5)-Cu(2)-Cl(1)	178.4(1)

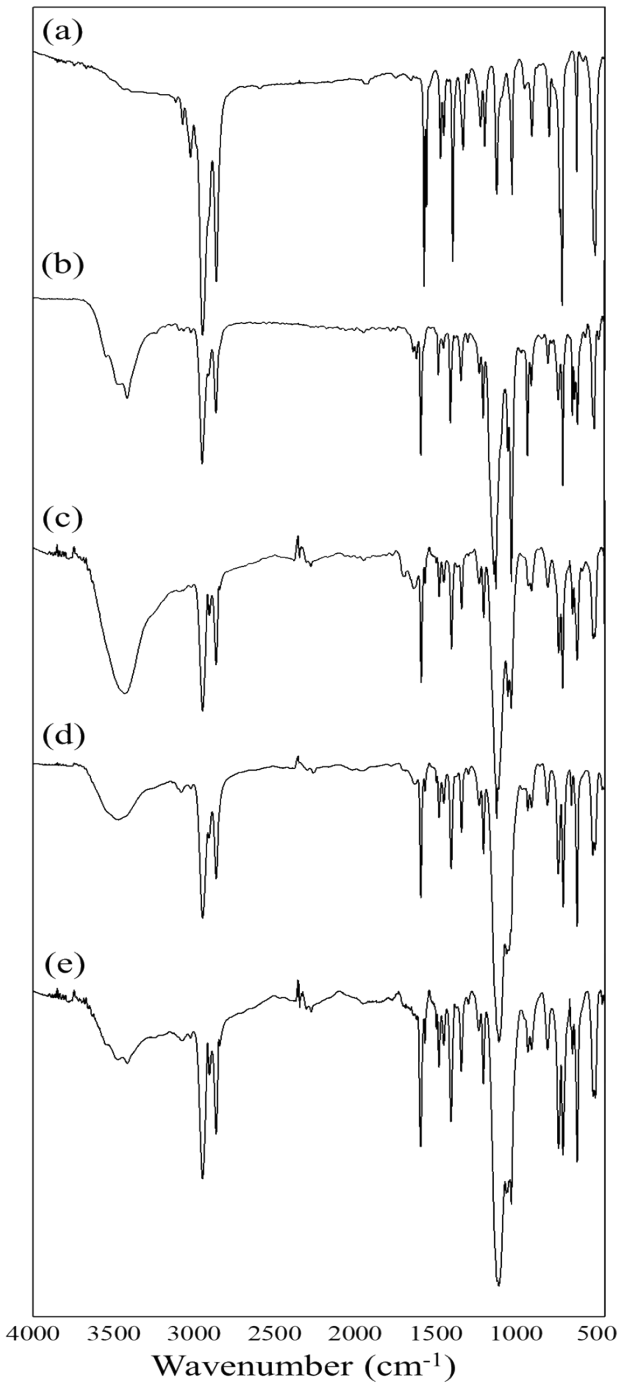

Fig. S1 IR spectra of L (a), $[Mn_6(ClO_4)_4(CH_3CN)_2(H_2O)_6L_{12}]8ClO_4 \cdot CH_3CN \cdot 7C_7H_8$ (b), $[Co_6(ClO_4)_4(CH_3CN)_7(H_2O)L_{12}][Co_6(ClO_4)_4(CH_3CN)_5(H_2O)_3L_{12}]16ClO_4 \cdot 6C_7H_8$ (c), $[Cu_6(ClO_4)_8(CH_3CN)_4L_{12}]4ClO_4 \cdot 5C_7H_8$ (d), and $[Zn_6(ClO_4)_4(CH_3CN)_2(H_2O)_6L_{12}]8ClO_4 \cdot CH_3CN \cdot 5C_7H_8$ (e).

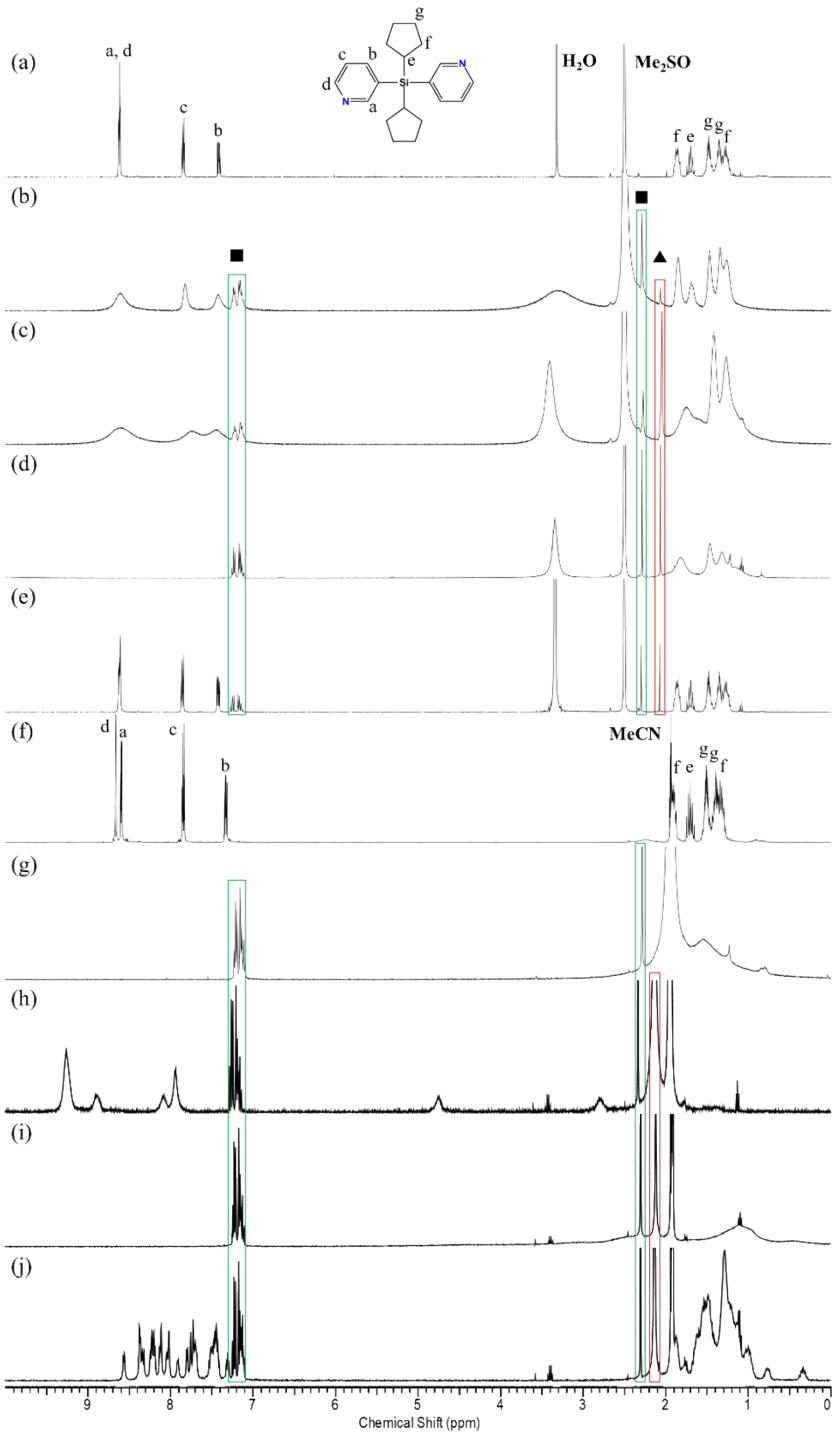

Fig. S2 ^{1}H NMR spectra of L (a, f), $[Mn_6(ClO_4)_4(CH_3CN)_2(H_2O)_6L_{12}]8ClO_4{\cdot}CH_3CN{\cdot}7C_7H_8$ (b, g), $[Co_6(ClO_4)_4(CH_3CN)_7(H_2O)L_{12}][Co_6(ClO_4)_4(CH_3CN)_5(H_2O)_3L_{12}]16ClO_4{\cdot}6C_7H_8$ (c, h), $[Cu_6(ClO_4)_8(CH_3CN)_4L_{12}]4ClO_4{\cdot}5C_7H_8$ (d, i), and $[Zn_6(ClO_4)_4(CH_3CN)_2(H_2O)_6L_{12}]8ClO_4{\cdot}CH_3CN{\cdot}5C_7H_8$ (e, j) in Me_2SO-d_6 (dissociated; a - f) and CD_3CN (dissolved; g - j). Square and triangle indicate toluene and acetonitrile, respectively.

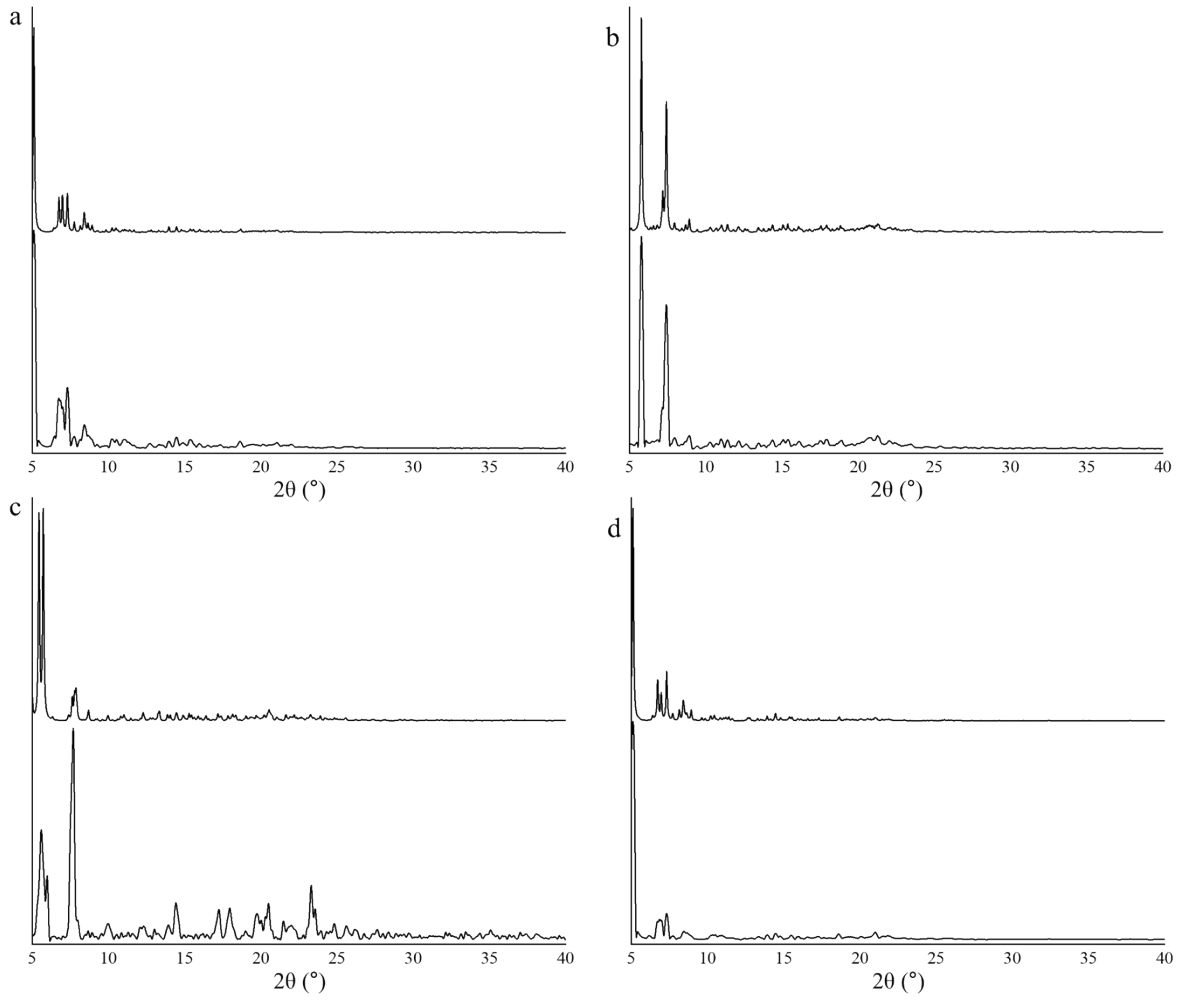

Fig. S3 PXRD patterns obtained through calculations (top) and experiments (bottom) in $[Mn_6(ClO_4)_4(CH_3CN)_2(H_2O)_6L_{12}]8ClO_4 \cdot CH_3CN \cdot 7C_7H_8$ (a), $[Co_6(ClO_4)_4(CH_3CN)_7(H_2O)L_{12}][Co_6(ClO_4)_4(CH_3CN)_5(H_2O)_3L_{12}]16ClO_4 \cdot 6C_7H_8$ (b), $[Cu_6(ClO_4)_8(CH_3CN)_4L_{12}]4ClO_4 \cdot 5C_7H_8$ (c), and $[Zn_6(ClO_4)_4(CH_3CN)_2(H_2O)_6L_{12}]8ClO_4 \cdot CH_3CN \cdot 5C_7H_8$ (d).

(a)

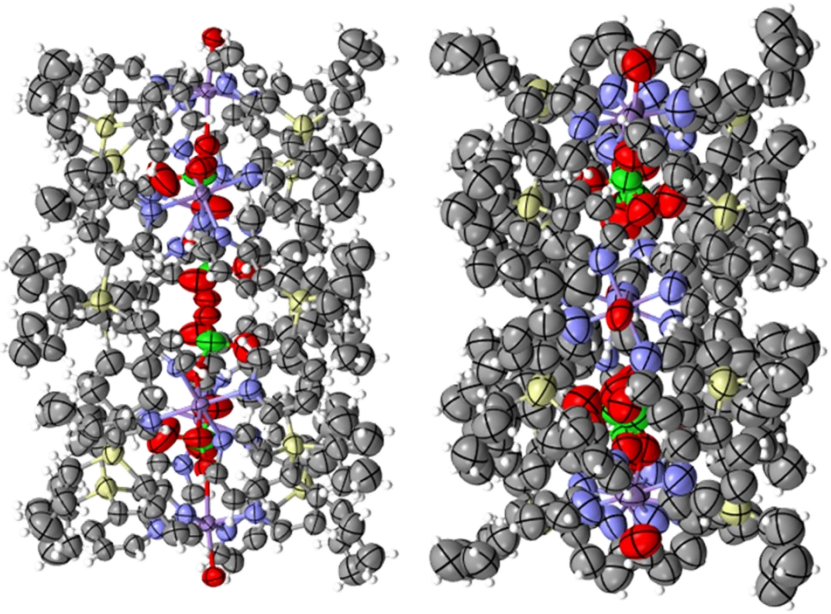

(b)

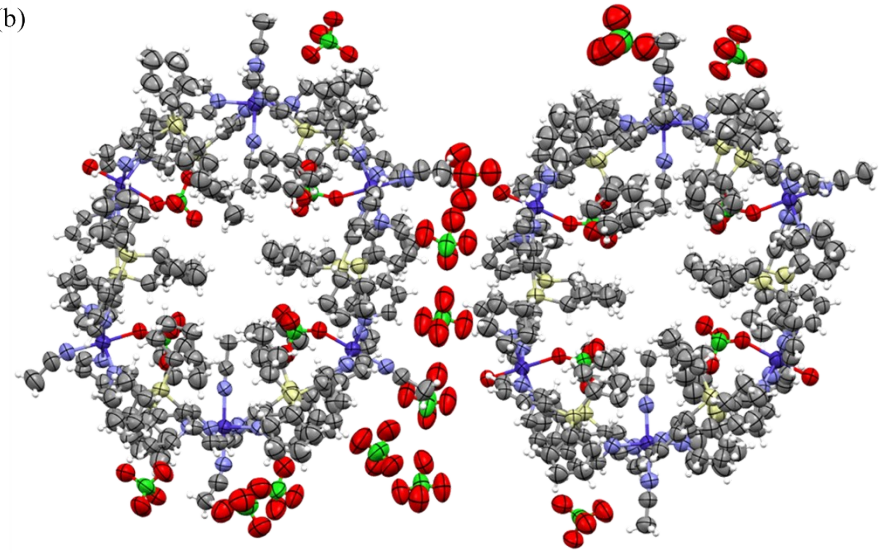

(c)

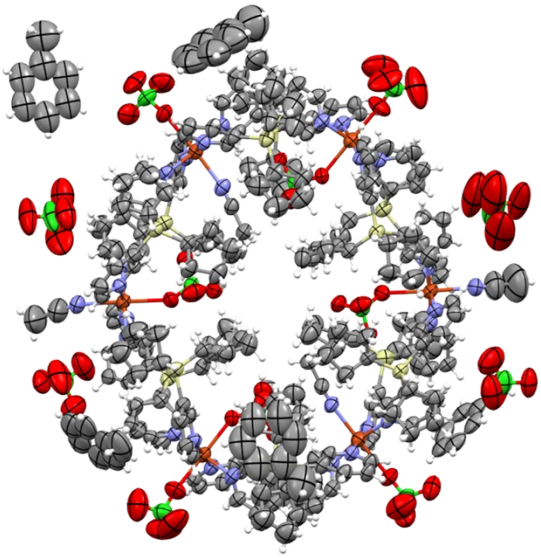

(d)

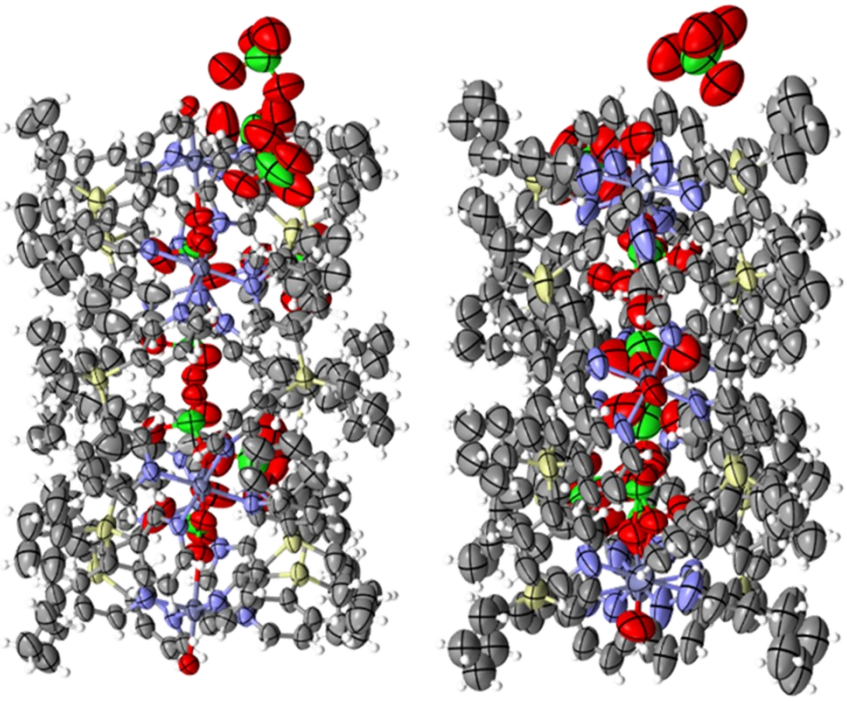

(e)

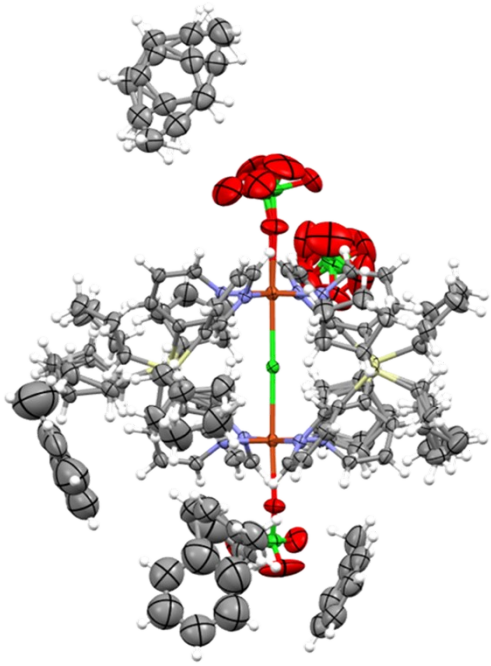

Fig. S4 The ellipsoidal model of $[Mn_6(ClO_4)_4(CH_3CN)_2(H_2O)_6L_{12}]8ClO_4{\cdot}CH_3CN{\cdot}7C_7H_8$ (a), $[Co_6(ClO_4)_4(CH_3CN)_7(H_2O)L_{12}][Co_6(ClO_4)_4(CH_3CN)_5(H_2O)_3L_{12}]16ClO_4{\cdot}6C_7H_8$ (b), $[Cu_6(ClO_4)_8(CH_3CN)_4L_{12}]4ClO_4{\cdot}5C_7H_8$ (c), $[Zn_6(ClO_4)_4(CH_3CN)_2(H_2O)_6L_{12}]8ClO_4{\cdot}CH_3CN{\cdot}5C_7H_8$ (d), and $[Cl@Cu_2(ClO_4)_2L_4]ClO_4{\cdot}4C_7H_8$ (e).

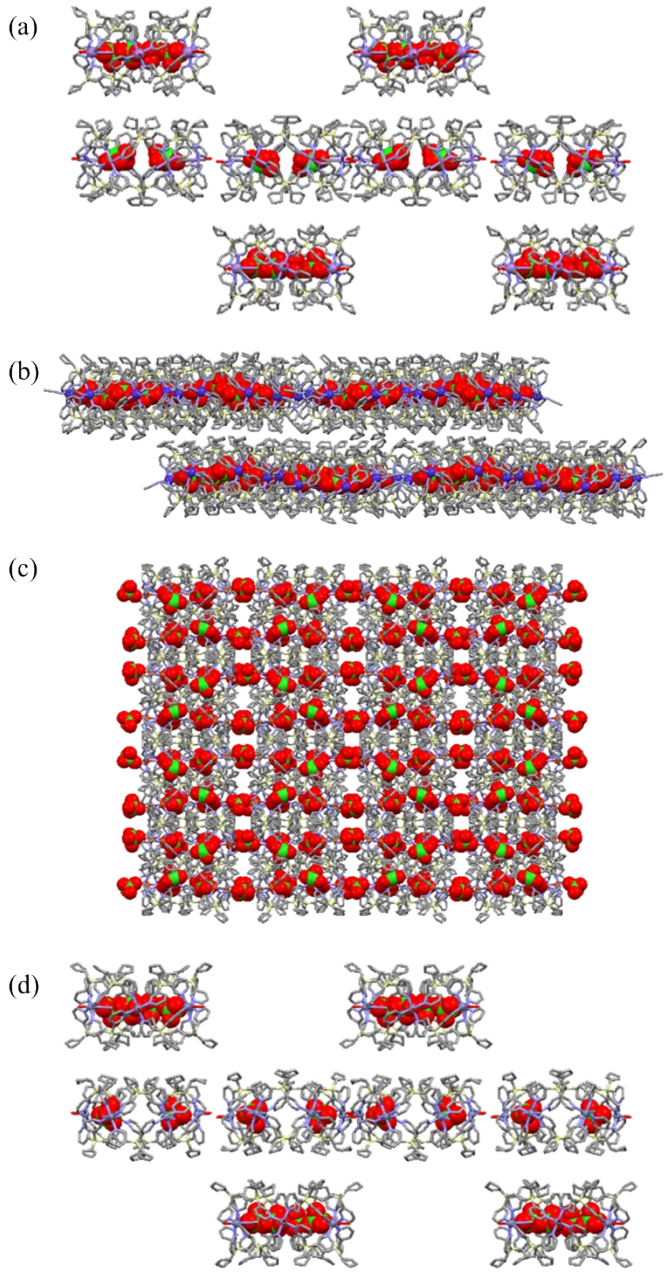

Fig. S5 The packing modes(top view) for $[Mn_6(ClO_4)_4(CH_3CN)_2(H_2O)_6L_{12}]8ClO_4{\cdot}CH_3CN{\cdot}7C_7H_8$ (a), $[Co_6(ClO_4)_4(CH_3CN)_7(H_2O)L_{12}][Co_6(ClO_4)_4(CH_3CN)_5(H_2O)_3L_{12}]16ClO_4{\cdot}6C_7H_8$ (b), $[Cu_6(ClO_4)_8(CH_3CN)_4L_{12}]4ClO_4{\cdot}5C_7H_8$ (c), and $[Zn_6(ClO_4)_4(CH_3CN)_2(H_2O)_6L_{12}]8ClO_4{\cdot}CH_3CN{\cdot}5C_7H_8$ (d).

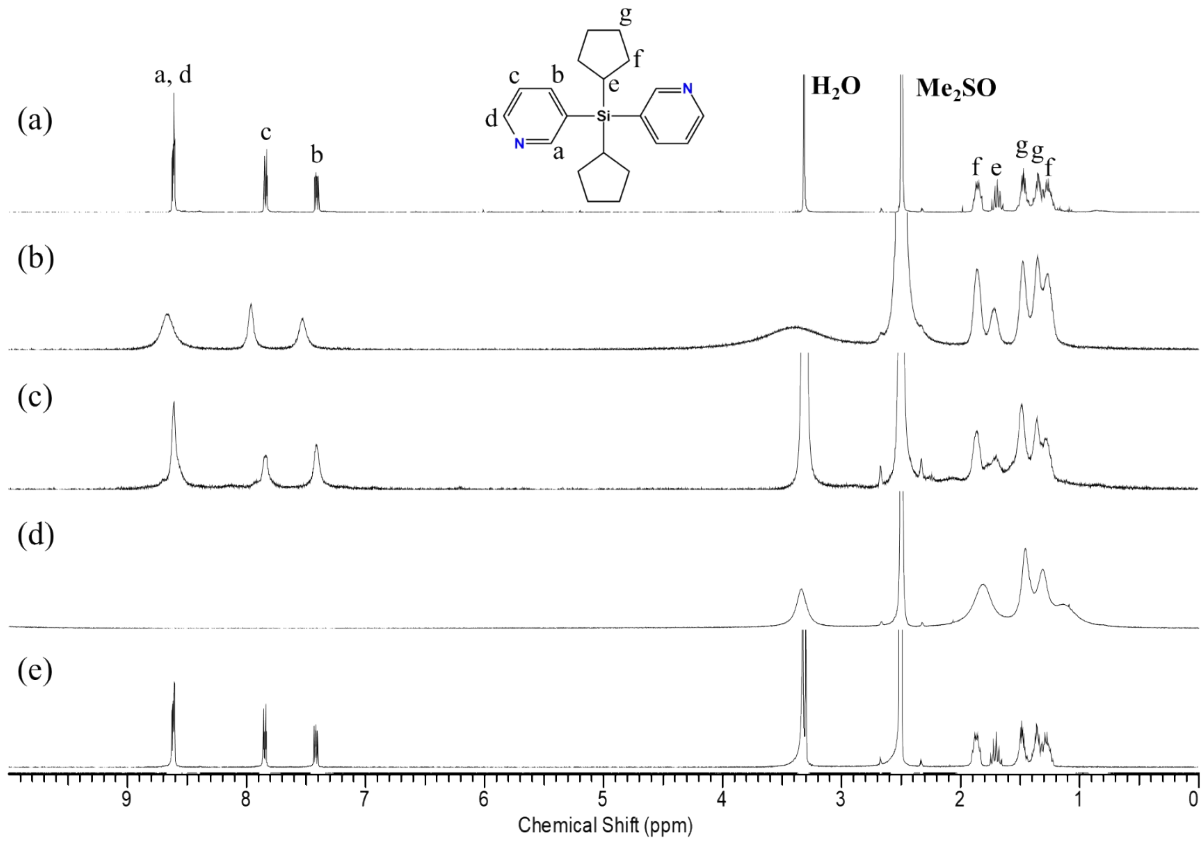

Fig. S6 ^{1}H NMR spectra of L (a), $[Mn(ClO_4)_2L_2]_n$ (b), $[Co(ClO_4)_2L_2]_n$ (c), $[Cu(ClO_4)_2L_2]_n$ (d), and $[Zn(ClO_4)_2L_2]_n$ (e) after heating up to 170 ^{o}C.

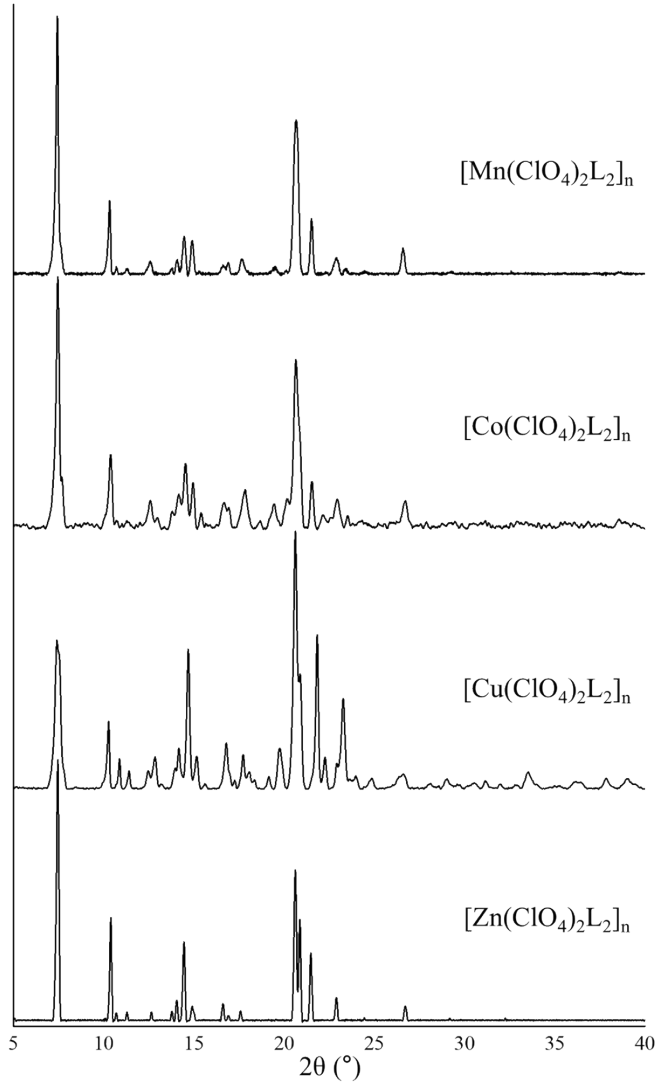

Fig. S7 PXRD patterns of $[Mn(ClO_4)_2L_2]_n$, $[Co(ClO_4)_2L_2]_n$, $[Cu(ClO_4)_2L_2]_n$, and $[Zn(ClO_4)_2L_2]_n$ after heating up to 170 °C.

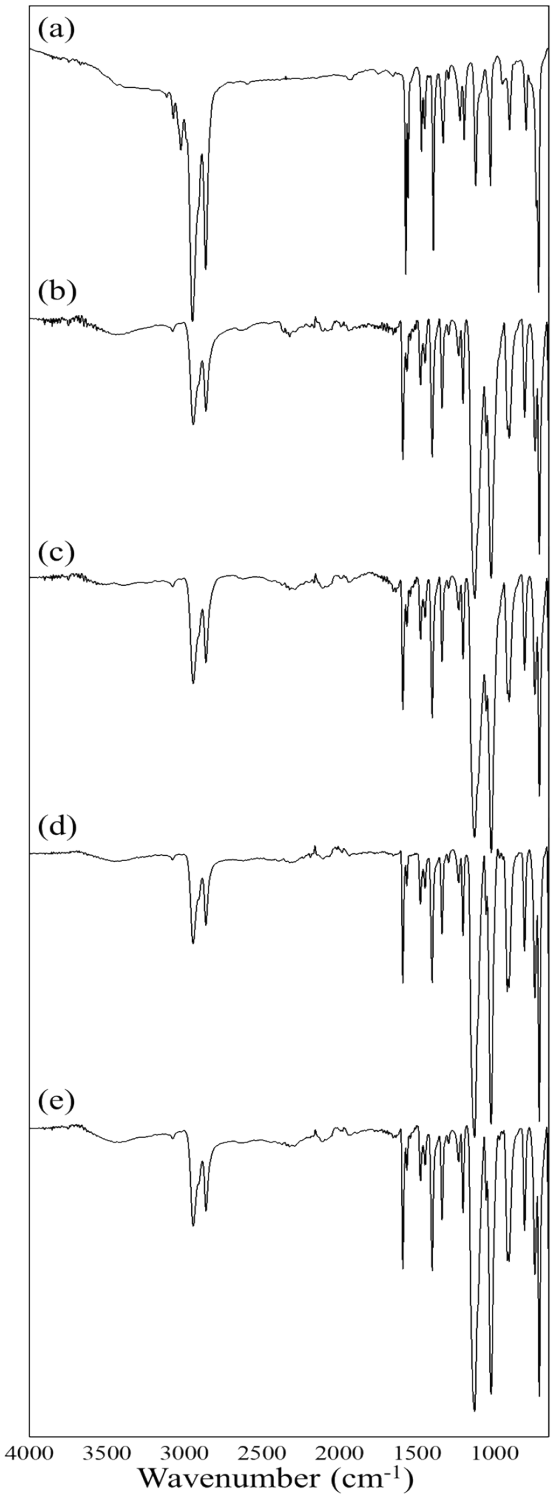

Fig. S8 IR spectra of L (a), $[Mn(ClO_4)_2L_2]_n$ (b), $[Co(ClO_4)_2L_2]_n$ (c), $[Cu(ClO_4)_2L_2]_n$ (d), and $[Zn(ClO_4)_2L_2]_n$ (e) after heating up to 170 °C.

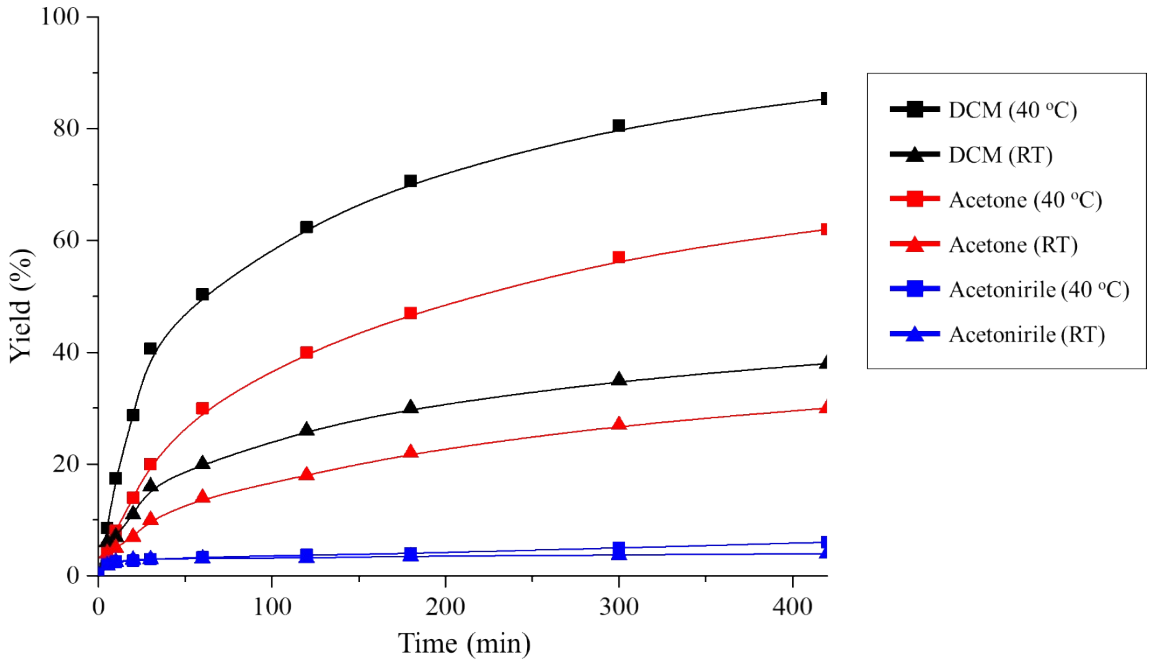

Fig. S9 The homogeneous catalysis rates of 3,5-di-*tert*-butylcatechol using $[Cu_6(ClO_4)_8(CH_3CN)_4L_{12}]4ClO_4 \cdot 5C_7H_8$ in dichloromethane (black line), acetone (red line), and acetonitrile (blue line) at 40 °C (square) and RT (triangle).

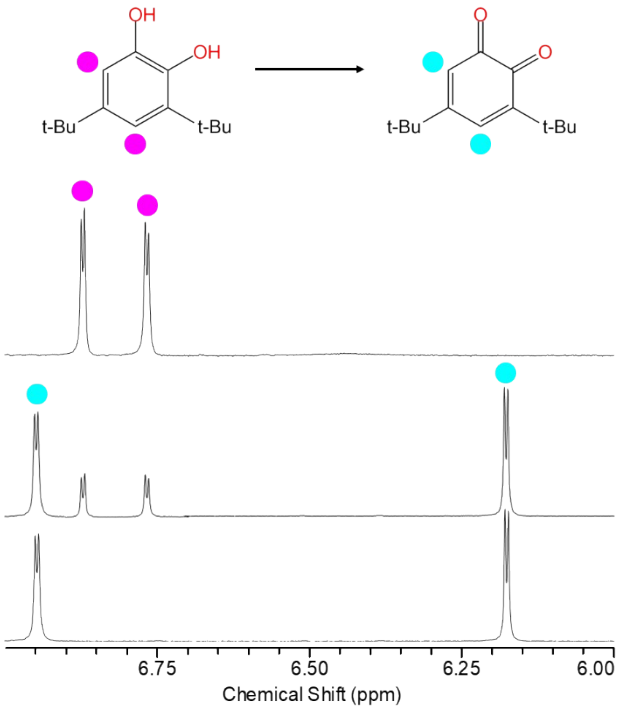

Fig. S10 ^{1}H NMR spectral procedure on catalytic oxidation 3,5-di-*tert*-butylcatechol to 3,5-di-*tert*-butylorthoquinone using $[Cu_6(ClO_4)_8(CH_3CN)_4L_{12}]4ClO_4 \cdot 5C_7H_8$ in dichoromethane-d_2.

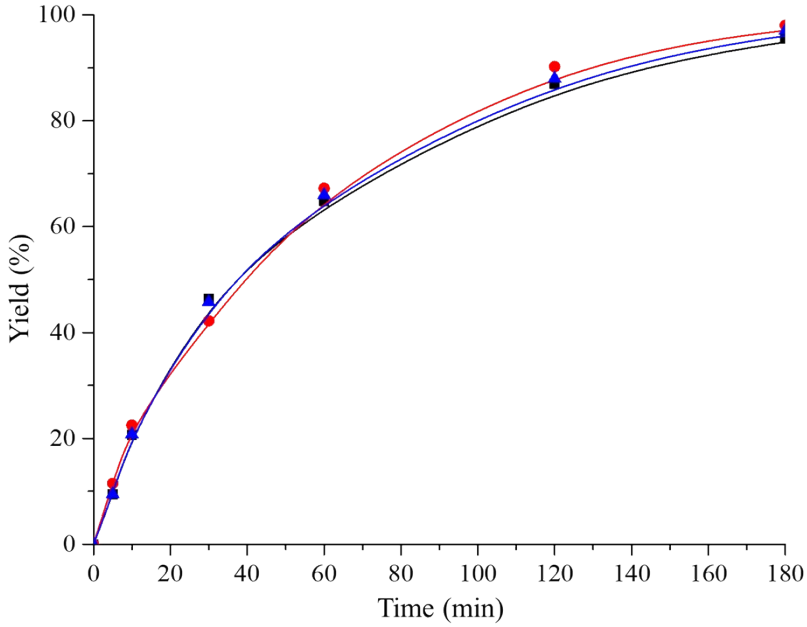

Fig. S11 Plot showing catalytic yields of transesterification of phenyl acetate using $[Zn_6(ClO_4)_4(CH_3CN)_2(H_2O)_6L_{12}]8ClO_4{\cdot}CH_3CN{\cdot}5C_7H_8$ (black line), $[Zn(ClO_4)_2L_2]$ (red line), and $Zn(ClO_4)_2$ + L (blue line) in methanol at 50 °C.

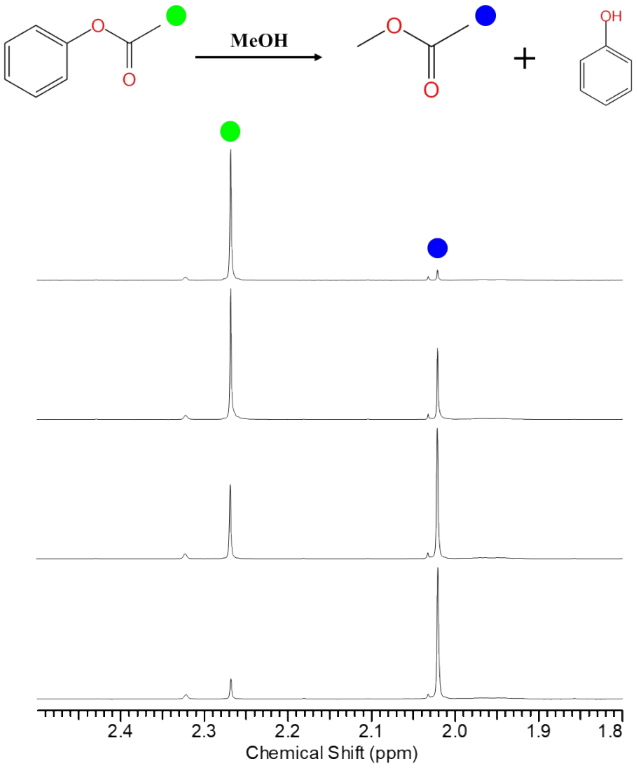

Fig. S12 ^{1}H NMR spectral procedure on transesterification of phenyl acetate using $[Zn_6(ClO_4)_4(CH_3CN)_2(H_2O)_6L_{12}]8ClO_4{\cdot}CH_3CN{\cdot}5C_7H_8$ in methanol at 50 ^{o}C.